Structure and interfacial properties of chicken apolipoprotein A-IV

Richard B. Weinberg,[1,*] Rachel A. Anderson,[*] Victoria R. Cook,[*] Florence Emmanuel,[†] Patrice Denefle,[§] Marcela Hermann,[**] and Armin Steinmetz[**]

Section of Gastroenterology,[*] Department of Internal Medicine, Wake Forest University School of Medicine, Winston-Salem, NC 27157; Cardiovascular Department,[†] Gencell Division, and Evry Genomics Center,[§] Aventis Pharma, 94403 Vitry sur Seine, France; and Department of Molecular Genetics,[**] Institute of Medical Biochemistry, University and Biocenter Vienna, A-1030 Vienna, Austria

Abstract **To gain insight into the evolution and function of apolipoprotein A-IV (apoA-IV) we compared structural and interfacial properties of chicken apoA-IV, human apoA-IV, and a recombinant human apoA-IV truncation mutant lacking the carboxyl terminus. Circular dichroism thermal denaturation studies revealed that the thermodynamic stability of the α-helical structure in chicken apoA-IV (ΔH = 71.0 kcal/mol) was greater than that of human apoA-IV (63.6 kcal/mol), but similar to that of human apoA-I (73.1 kcal/mol). Fluorescence chemical denaturation studies revealed a multiphasic red shift with a 65% increase in relative quantum yield that preceded loss of α-helical structure, a phenomenon previously noted for human apoA-IV. The elastic modulus of chicken apoA-IV at the air/water interface was 13.7 mN/m, versus 21.7 mN/m for human apoA-IV and 7.6 mN/m for apoA-I. The interfacial exclusion pressure of chicken apoA-IV for phospholipid monolayers was 31.1 mN/m, versus 33.0 mN/m for human A-I and 28.5 mN/m for apoA-IV. We conclude that the secondary structural features of chicken apoA-IV more closely resemble those of human apoA-I, which may reflect the evolution of apoA-IV by intraexonic duplication of the apoA-I gene. However, the interfacial properties of chicken apoA-IV are intermediate between those of human apoA-I and apoA-IV, which suggests that chicken apoA-IV may represent an ancestral prototype of mammalian apoA-IV, which subsequently underwent further structural change as an evolutionary response to the requisites of mammalian lipoprotein metabolism.**—Weinberg, R. B., R. A. Anderson, V. R. Cook, F. Emmanuel, P. Denefle, M. Hermann, and A. Steinmetz. **Structure and interfacial properties of chicken apolipoprotein A-IV.** ***J. Lipid Res.*** **2000.** 41: **1410–1418.**

Supplementary key words surface tension • interfacial elasticity • monolayers • fluorescence • spectroscopy • molecular evolution

Apolipoprotein A-IV (apoA-IV) is a 46-kDa plasma protein (1), making it the largest member of a family of lipid-binding proteins that regulate plasma lipoprotein metabolism (2). In mammals, apoA-IV is synthesized by the intestinal enterocytes (3) during lipid absorption (4), and enters the circulation on the surface of nascent chylomicrons (5). Sequence analysis of the apolipoprotein multigene family predicts that apoA-IV is the most recently evolved apolipoprotein, and probably originated by intraexonic duplication of the apoA-I gene ~270–307 million years ago (2, 6). Although many physiologic functions have been proposed for apoA-IV, the preponderance of evidence suggests that its primary role is the regulation of intestinal lipid absorption and chylomicron assembly (7).

ApoA-IV has several distinctive structural features. The amino acid sequence of apoA-IV is punctuated by proline-containing β turns (8), and the amphipathic α helices in apoA-IV are hydrophilic (9) and have a radial charge distribution (10) that precludes deep penetration into condensed lipid monolayers (11, 12). Consequently, apoA-IV has the weakest lipid affinity (13, 14) and the lowest interfacial exclusion pressure (15) of any apolipoprotein. The C terminus of apoA-IV contains a unique and highly conserved tetrapeptide repeat with the sequence EQ(Q/A/V)Q (8). This region is the site of murine (16), baboon (17), and human (18, 19) genetic polymorphisms that affect apoA-IV structure (12), plasma lipid levels (reviewed in ref. 20), and the response to diet (17, 21–23).

We have identified a 38-kDa avian homolog of mammalian apoA-IV (24). Like mammalian apoA-IV, chicken apoA-IV is synthesized primarily in the intestine, contains no N-linked glycosylation sites, is predicted to contain multiple amphipathic α-helical domains, binds to lipid, and weakly activates lecithin–cholesterol acyltransferase in vitro. However, chicken apoA-IV differs significantly from human apoA-IV in that it is a much more hydropho-

Abbreviations: apo, apolipoprotein; DMPC, l-α-dimyristoyl phosphatidylcholine; EDTA, ethylenediaminetetraacetic acid; EPC, egg phosphatidylcholine; GdmHCl, guanadinium hydrochloride; HPLC, high pressure liquid chromatography; NATA, *N*-acetyl tryptophanamide; PBS, phosphate-buffered saline; SDS-PAGE, sodium dodecyl sulfate-polyacrylamide gel electrophoresis.

[1] To whom correspondence should be addressed.

bic protein, has longer α-helical hydrophobic domains and shorter hydrophilic domains, and its primary structure is truncated at 346 amino acids, and hence lacks the unique mammalian C-terminal repeated EQQQ motif. This suggests that chicken apoA-IV could be the molecular ancestor of mammalian apoA-IV, and that the mammalian apoA-IV C-terminal domain may be a structural adaptation that evolved to confer a new physiologic function to this apolipoprotein. Therefore, to gain further insight into the evolution of mammalian apoA-IV and its role in lipoprotein metabolism, we used spectroscopic and dynamic interfacial techniques to examine the structural and functional differences among chicken apoA-IV, human apoA-IV, human apoA-I, and a recombinant human apoA-IV truncation mutant lacking the C terminus.

MATERIALS AND METHODS

Phospholipids and apolipoproteins

Egg phosphatidylcholine (EPC) and l-α-dimyristoyl phosphatidylcholine (DMPC) were obtained from Sigma (St. Louis, MO), dissolved in high performance liquid chromatography (HPLC)-grade chloroform (Aldrich, Milwaukee, WI), and stored under nitrogen at −20°C. Phospholipid concentration was determined by phosphorus analysis (25). Phospholipids were >99% pure by thin-layer chromatography (TLC) on silica gel. Human apoA-IV was isolated from donors homozygous for the A-IV-1 allele by adsorption from lipoprotein-depleted plasma to a phospholipid-triglyceride emulsion (26). Chicken apoA-IV was isolated from chicken plasma (24). Recombinant human apoA-IV lacking the terminal 44 amino acids (apoA-IV-ΔC44) was created by site-directed mutagenesis of a plasmid containing the human apoA-IV coding sequence, insertion of the sequence between the *Bam*HI and *Nde*I sites of the pET-3a vector, and expression in *Escherichia coli* BL21(DE3)(pLys) (27). Recombinant apoA-IV accumulated in *E. coli* in high density cell culture at levels up to 5–10% of total bacterial protein. Human apoA-I was isolated from high density lipoproteins (28). Protein concentration of apolipoprotein solutions was determined with bicinchoninic acid (29). All apolipoprotein preparations, including apoA-IV-ΔC44, were homogeneous by sodium dodecyl sulfate-polyacrylamide gel electrophoresis (SDS-PAGE).

Computational analysis of apolipoprotein A-IV structure

The structure of chicken and human apoA-IV was analyzed by Fourier transformation of mean residue helical hydrophobic moment versus residue rotation angle along the protein sequences (30), using a consensus residue hydrophobicity scale (31). Nonconservative sequence variability between chicken apoA-IV and four mammalian apoA-IV sequences (human, baboon, rat, and mouse) and the difference in residue hydrophobicity between chicken and human apoA-IV were calculated by a substitution matrix-median filter algorithm (8).

Circular dichroism spectropolarimetry

Circular dichroism studies were performed on a JASCO (Tokyo, Japan) J-720 spectropolarimeter. Spectra of apolipoproteins at 3 μM in 50 mM Tris (pH 7.4), 1 mM EDTA, 0.02% sodium azide were recorded at 25°C from 190 to 260 nm using a 1-mm thermostatted cell, a 1-mm spectral band width, and a 2-sec time constant. Buffer blanks were digitally subtracted. Chemical denaturation studies were performed by sequential addition of aliquots of buffered 6 M guanidinium hydrochloride (GdmHCl). Mean residue ellipticity at 222 nm, percent α helicity, and the free energy of stabilization, ΔG_0, were calculated as previously described (14). Thermal denaturation studies were performed by measuring ellipticity at 222 nm as a function of temperature from 20 to 65°C. The enthalpy of denaturation, ΔH, and the temperature at the thermal denaturation midpoint, T_m, were determined from the slope of plots of ΔG versus 1/T (32).

Fluorescence spectroscopy

Fluorescence studies were performed on an SLM 8000C spectrofluorometer (Spectronic Unicam, Rochester, NY). Spectra of apolipoproteins at 3 μM in 50 mM Tris (pH 7.4), 1 mM EDTA, 0.02% sodium azide were recorded at 25°C from 290 to 370 nm with a stirred, thermostatted 1-cm cell with excitation at 280 nm, a 1-sec integration rate, and 4-nm slits on both excitation and emission monochromators. Spectra were excitation corrected by reference to a rhodamine quantum counter, and corrected for scatter and Raman emission by digital subtraction of buffer blanks. Denaturation studies were performed by sequential addition of aliquots of buffered 6 M GdmHCl. Fluorescence quenching studies were performed by addition of aliquots of buffered 6 M KI. Stern-Volmer quenching constants, K_q, were obtained from plots of I_o/I versus [KI]; fractional tryptophan exposure was calculated as the ratio of K_q (apolipoprotein) to K_q (*N*-acetyl tryptophanamide) (33).

Dynamic interfacial properties at the air/water interface

The dynamic interfacial properties of apolipoproteins at the air/water interface were examined with a pulsating bubble surfactometer (Electronetics, Amherst, NY). This instrument sinusoidally oscillates a tiny air bubble in a chamber filled with aqueous sample, records bubble pressure (P) as a function of bubble radius (r), and calculates interfacial tension (γ) from the Young-Laplace equation, $\Delta P = 2\gamma/r$ (34). Studies were conducted at 25°C with apolipoproteins at 0.4 mg/mL in 50 mM Tris, 100 mM NaCl (pH 7.5). Surface area (A)−γ loops were recorded at 20 cycles/min. Surface pressure at the air/water interface was taken as $\gamma_{buffer} - \gamma_{sample}$. Absolute elasticity (ε) was calculated as $\Delta\gamma/(\Delta A/A)$; the viscoelastic component (ε_v) was calculated as $\varepsilon \sin(\phi)$, where ϕ is the phase angle of the A−γ loops (35).

Interfacial exclusion pressure at the phospholipid/water interface

The interfacial exclusion pressure at the phospholipid/water interface was determined with a KSV Instruments (Helsinki, Finland) 5000 Langmuir film balance, enclosed in a cabinet maintained at 25°C and 70–75% relative humidity (36). Magnetically stirred Teflon wells were filled with 50 mL of degassed phosphate-buffered saline (PBS), and the buffer surface was cleaned by vacuum aspiration. EPC monolayers were spread at the air/buffer interface to the desired initial pressure (Π_i) by dropwise addition of EPC in $CHCl_3$, and were left for 30 min to assure complete evaporation of organic solvent. Apolipoprotein solutions were injected into the subphase at concentrations determined to yield saturation binding to the interface. The change in interfacial pressure (ΔΠ) was continuously monitored with a Wilhelmy plate and electrobalance until it reached a stable plateau. The interfacial exclusion pressure (Π_{ex}) was determined by extrapolation of graphs of ΔΠ versus Π_i.

Light-scattering studies

Light-scattering studies were performed with a Perkin-Elmer (Foster City, CA) Lambda 20 UV/visible (UV/Vis) spectrometer and 10-mm cells thermostatted by a Lauda RM 6 water circulator. The binding kinetics of apolipoproteins to DMPC multilamellar vesicles at 24°C was examined by monitoring the time-depen-

dent decrease in absorbance at 350 nm after the addition of apolipoproteins at a 1:50 protein/phospholipid molar ratio (37). This technique measures the decrease in light scattering consequent to dissolution of large multilamellar vesicles into smaller DMPC/apolipoprotein micellar complexes. Exponential binding rate constants were calculated from log transformation of the absorbance versus time curves. Data presented are the means ± SE for four (chicken apoA-IV) or five (human apoA-I and apoA-IV) separate experiments.

RESULTS

Computational analysis of apolipoprotein A-IV structure

Fourier transformation of mean residue helical hydrophobic moment as a function of residue rotation angle along a protein sequence identifies regions of α-helical structure as maxima between 80 and 120°, β-sheet structure as maxima between 140 and 180°, and random coil

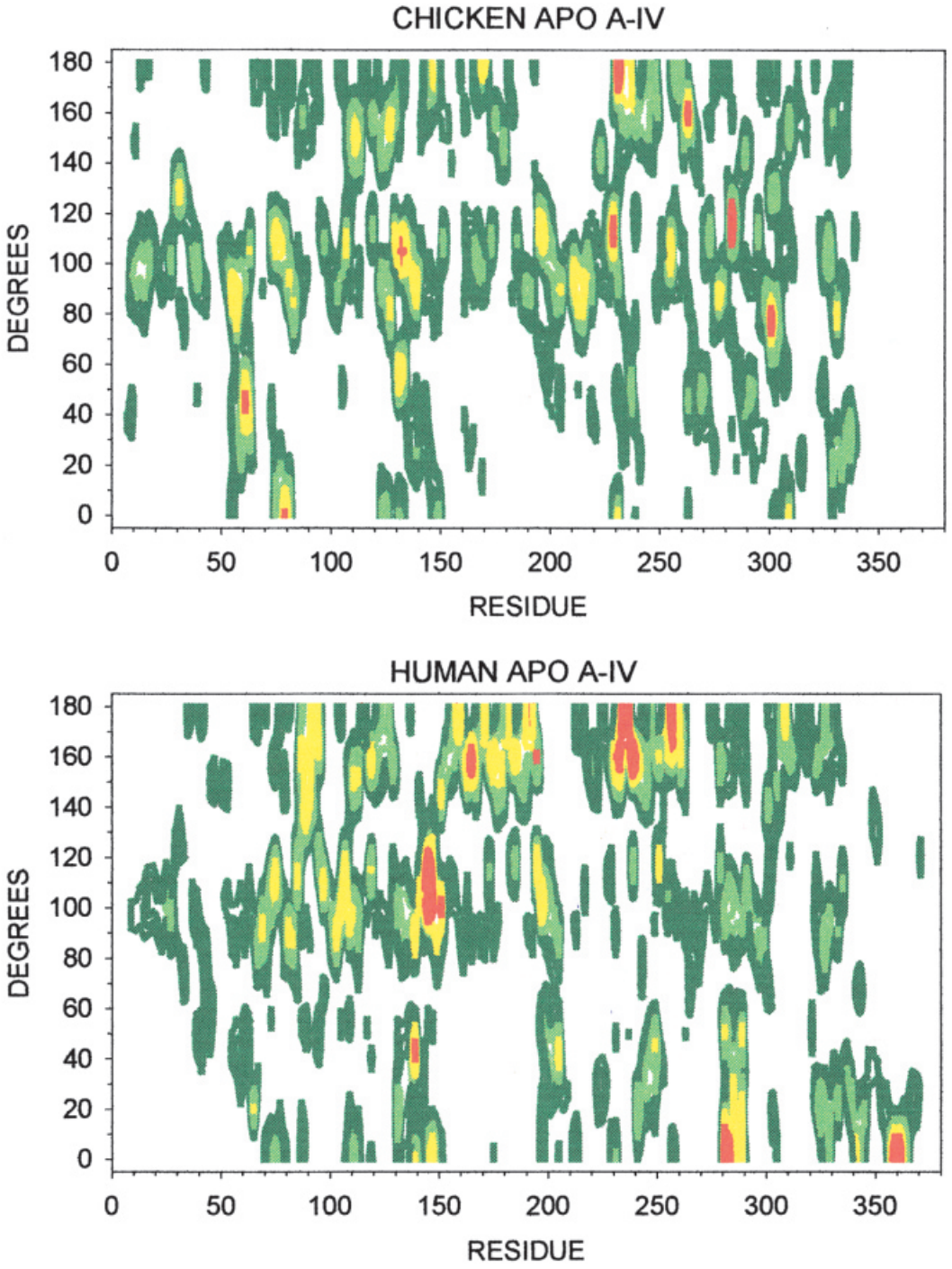

Fig. 1. Fourier transform plots of mean residue helical hydrophobic moment (contour color) versus residue rotation angle (y axis) along the amino acid sequence (x axis) of chicken and human apolipoprotein A-IV. Contour colors correspond to the mean helical hydrophobic moment: white, 0–4.49 kcal/mol; dark green, 4.50–5.99 kcal/mol; light green, 6.00–6.99 kcal/mol; yellow, 7.00–7.99 kcal/mol; red, >8.00 kcal/mol.

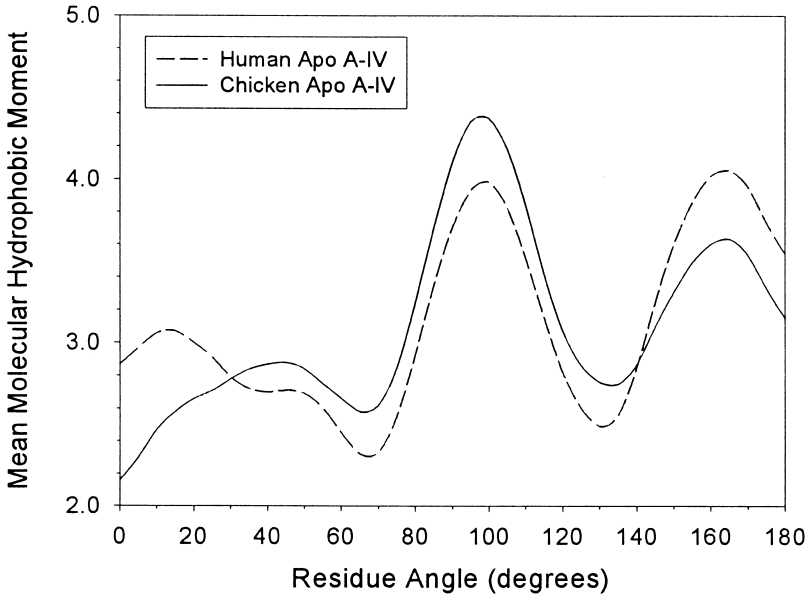

Fig. 2. Mean molecular hydrophobic moment versus residue angle for chicken and human apolipoprotein A-IV. The plot was derived from the data sets in Fig. 1 by averaging the mean residue helical hydrophobic moment across the entire molecule from 0 to 180°.

structure as maxima between 0 and 40° (30). This analysis of chicken and human apoA-IV sequences revealed that, overall, chicken apoA-IV has a much better defined α-helical structure than human apoA-IV (**Fig. 1**), and a higher mean hydrophobic moment across the entire molecule, with a maximum at 99° (**Fig. 2**). A break in the strong repeated α-helical pattern present in the amino-terminal half of the apoA-IV molecule was evident near residue 230 in both chicken and human apoA-IV; this may be a molecular footprint of the elongation of the ancestral apoA-I molecule. In chicken apoA-IV a predominant secondary structure pattern was less well defined from residue 230 to the carboxyl terminus, whereas in human apoA-IV it was better organized with alternating regions of strong β-sheet maxima between residues 230 and 265, and α-helix maxima between residues 270 and 300. The C terminus of human apoA-IV displayed strong maxima at 0–20°, suggestive of random coil structure. Comparison of chicken and mammalian apoA-IV sequences revealed hydrophilic residue substitutions across the entire molecule, although the greatest nonconservative substitutions were present toward the carboxyl terminus between residues 220 and 315

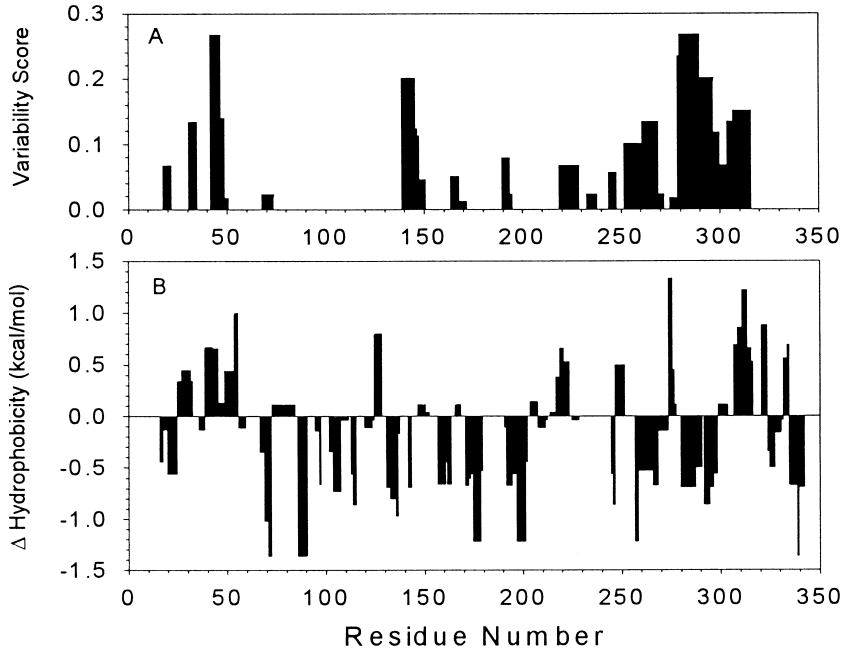

Fig. 3. (A) Residue variability between chicken apoA-IV and four mammalian apoA-IV sequences (human, baboon, rat, mouse) calculated with a substitution matrix-median filter algorithm (8). (B) Difference in hydrophobicity between chicken and human apoA-IV calculated for individual residues and passed through a median filter (8). Negative values denote domains where the human sequence is more hydrophilic.

TABLE 1. Spectroscopic and thermodynamic properties

	Length	α Helix	ΔH^0	T_m	λ_{max}	K_q/K_q^{nata}
	Residue #	*%*	*kcal/mol*	*°C*	*nm*	
Human apoA-I	1–243	54[a]	73.1	57.9	333[a]	0.29[a]
Chicken apoA-IV	1–346	55	71.0	54.1	333	0.15
Human apoA-IV-1	1–376	56[b]	63.6	48.1	332	0.24[c]
Human apo A-IVΔC44	1–332	57	29.9	48.0	338	0.12

[a] Weinberg and Spector, 1985 (14); [b] Weinberg, Jordan, and Steinmetz, 1990 (12); [c] Weinberg, 1988 (33).

(**Fig. 3**). Together these findings suggest that the carboxyl-terminal half of apoA-IV has undergone a more rapid evolutionary change in primary and secondary structure since the divergence of avians and mammals.

Spectroscopic studies

Circular dichroism spectra of native chicken apoA-IV showed a mean residue ellipticity of 18,517 deg·cm²/dmol at 222 nm, which corresponds to 55% α-helical structure. C-terminal truncation of human apoA-IV had little effect on its native α helicity (**Table 1**), as might be expected given the predicted random coil structure of the C terminus. Compared with human apoA-IV (14), chicken apoA-IV was relatively resistant to chemical denaturation: the $[GdmHCl]^{50\%}$ was 1.3 M (**Fig. 4**), and the calculated free energy of stabilization was 4.9 kcal/mol, parameters similar to those obtained for human apoA-I (14). Thermal denaturation of chicken apoA-IV (**Fig. 5**) yielded an enthalpy of denaturation, ΔH_D^0, of 71.0 kcal/mol with a transition midpoint of 54.1°C, values that, again, were closer to those of human apoA-I than human apoA-IV. The ΔH_D^0 of apoA-IVΔC44, 29.9 kcal/mol, was more than 50% lower than that of human apoA-IV, which suggests that this deletion significantly disrupted the stability of the molecule.

Fluorescence spectroscopy of chicken apoA-IV revealed several distinctive features previously observed with human apoA-IV. The fluorescence emission of its single amino-terminal tryptophan was blue shifted to 333 nm, and was highly resistant to iodide quenching, indicating that it resides in a hydrophobic environment. Moreover, chemical denaturation induced a multiphasic red shift in the wavelength of maximum fluorescence emission and a 65% increase in the relative quantum yield at 0.5 M GdmHCl (Fig. 4). We have proposed that these spectral phenomena indicate that the amino-terminal tryptophan in native apoA-IV resides in the hydrophobic interior of a loosely folded conformation within energy transfer range of nonvicinal tyrosine residues, and that the loss of tertiary structure precedes unfolding of the α-helical domains (33). The fluorescence emission of apoA-IVΔC44 was red shifted compared with the native protein, although iodide accessibility was lower. In light of the thermal denaturation data, these findings suggest that the C terminus, although hydrophilic, is important for the overall stability and folding of the apoA-IV molecule.

Interfacial properties at the air/water and lipid/water interface

The resting interfacial tension and surface pressure of chicken and human apoA-IV at the air/water interface were similar (**Table 2**). The ΔA–γ loops for both chicken and human apoA-IV displayed large changes in surface tension with changes in surface area, indicative of elastic behavior at the interface, and a large phase angle, indicative of a large viscous component (**Fig. 6**). These data establish that, like human apoA-IV (38), chicken apoA-IV can undergo rate-dependent changes in surface confor-

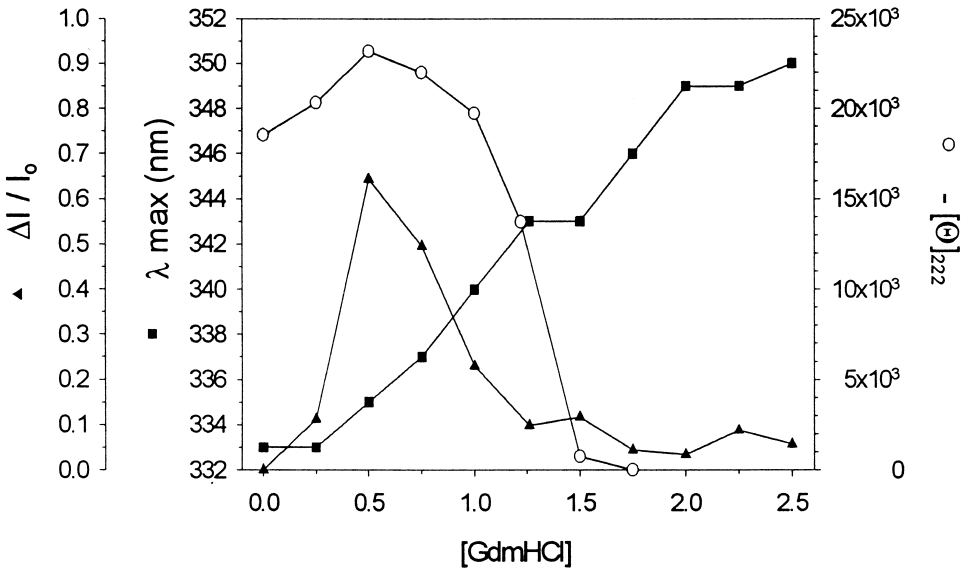

Fig. 4. Fluorescence and circular dichroism spectroscopy studies of the chemical denaturation of chicken apolipoprotein A-IV. The wavelength of maximum fluorescence emission (solid squares), the change in maximal fluorescence intensity from baseline (solid triangles), and the mean residue ellipticity at 222 nm (open circles) were determined as a function of guanidinium hydrochloride concentration.

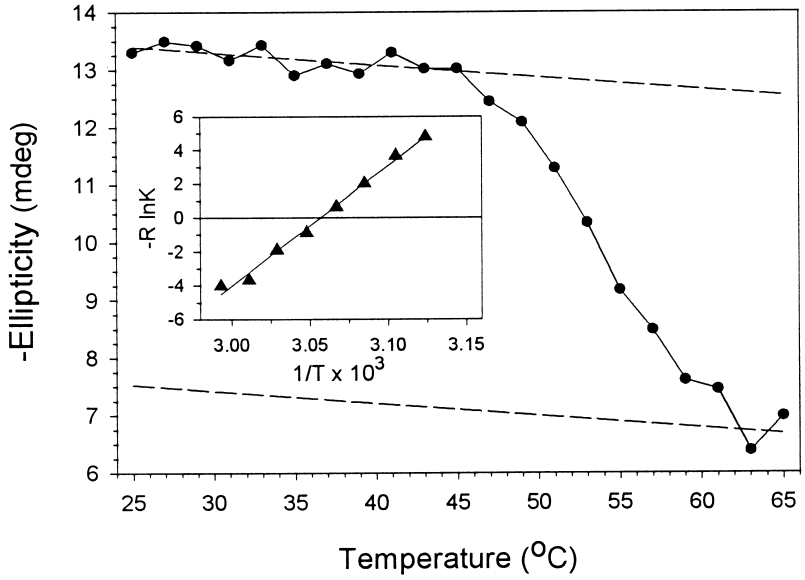

Fig. 5. Circular dichroism spectroscopy-thermal denaturation study of chicken apolipoprotein A-IV. Ellipticity at 222 nm was monitored as a function of temperature from 25 to 65°C. Inset: Van't Hoff plot of ΔG versus 1/T.

mation in response to changes in interfacial area, albeit with a lower elastic modulus than human apoA-IV. In contrast, apoA-I displayed lower resting interfacial tension, higher surface pressure, and significantly less interfacial elasticity than either chicken or human apoA-IV.

The binding of chicken apoA-IV to egg phosphatidylcholine monolayers, as evidenced as a change in surface pressure, decreased linearly with increasing initial pressure (data not shown); extrapolation of $\Pi_i - \Delta\Pi$ curves to zero revealed that chicken apoA-IV was excluded from the lipid/water interface at pressures above 31.1 mN/m. In comparison, the exclusion pressure was 28.5 mN/m for human apoA-IV, 29.0 mN/m for apoA-IV-ΔC44, and 33.0 mN/m for apoA-I. These data suggest that the hydrophilic C terminus of human apoA-IV is not a determinant of its labile interfacial binding, and conversely, that the stronger binding of chicken apoA-IV is a function of its higher global hydrophobicity.

The kinetics of micellar solubilization of DMPC vesicles

Addition of chicken apoA-IV to DMPC multilamellar vesicles at 24°C caused a time-dependent decrease in absorbance at 350 nm (**Fig. 7**), which was due to the decrease in light scattering consequent to the dissolution of the large multilamellar vesicles into much smaller DMPC/apolipoprotein micellar complexes. Biphasic kinetics were observed with a rate constant of 6.55×10^{-3} min^{-1} for the early phase (0–20 min) and 2.11×10^{-3} for the late phase (20–100 min). Human apoA-IV displayed similar curves and kinetics, with a rate constant of 6.18×10^{-3} min^{-1} for the early phase and 2.94×10^{-3} for the late phase. In contrast, human apoA-I displayed significantly more rapid early phase kinetics, with a rate constant of 1.46×10^{-2} min^{-1}; the late phase rate constant, 2.67×10^{-3}, was similar to that of apoA-IV. As micellar solubilization of DMPC multilamellar vesicles by apolipoproteins requires both binding to the vesicle surface and subsequent penetration of amphipathic helices into the phospholipid monolayer (37), these data suggest that, like human apoA-IV (11, 12, 33), the amphipathic helices in chicken apoA-IV are unable to deeply penetrate lipid interfaces.

TABLE 2 Interfacial properties at the air/water and phospholipid/water interface

	γ	Π	ε	ε_v	Π_{ex}
			mN/m		
Human apoA-I	39.8	32.0	7.6	1.6	33.0
Chicken apoA-IV	43.6	28.2	13.7	13.5	31.1
Human apoA-IV-1	42.5	29.3	21.7	10.2	28.5
Human apo A-IVΔC44	nd	nd	nd	nd	29.0

γ, Resting interfacial tension at the air/water interface; Π, resting surface pressure at the air/water interface; ε, interfacial elasticity; ε_v, viscous elastic component; Π_{ex}, exclusion pressure at the phospholipid/water interface; nd, not determined.

DISCUSSION

These data suggest that chicken apoA-IV is a unique apolipoprotein that in many of its structural and biophysical properties more closely resembles human apoA-I than human apoA-IV. As predicted from the analysis of the amino acid sequence, the circular dichroism studies found a high content of α-helical structure in chicken apoA-IV; however, its secondary structure was much more stable to chemical and thermal denaturation than human apoA-IV. The number of α helices in a globular protein usually contributes to the enthalpy of unfolding (39), yet the presence of additional α-helical domains in chicken apoA-IV did not raise its thermal stability beyond that of apoA-I. This may reflect the poor structural organization and relative hydrophilicity of the C-terminal half of the molecule. Thus, the stability of chicken apoA-IV may be due primarily to the well-organized hydrophobic helical structure of the N-terminal domains; conversely, the relatively low stability of human apoA-IV may be a consequence of hydrophilic residue substitutions across the en-

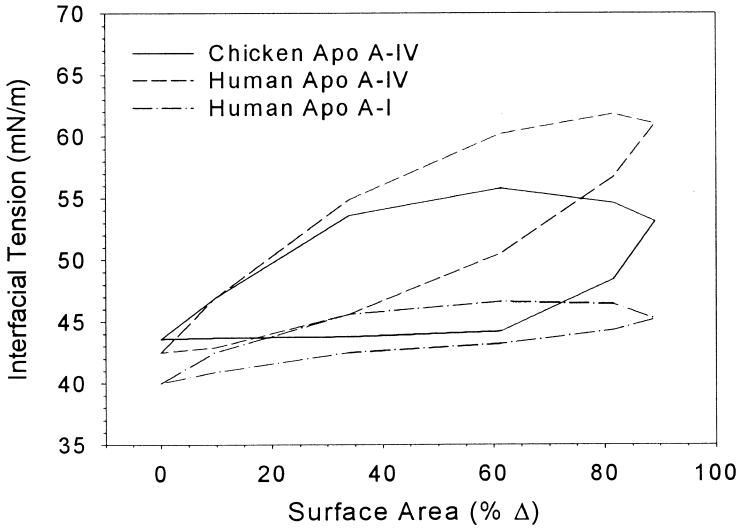

Fig. 6. Dynamic interfacial behavior of chicken apolipoprotein A-IV and human apolipoproteins A-IV and A-I. The surface tension of apolipoproteins at the air/water interface was measured in a pulsating bubble surfactometer as the bubble surface area was sinusoidally oscillated at 20 cycles/min.

tire molecule. Nonetheless, the value of ΔH for chicken apoA-IV is low compared with other globular proteins, which suggests that, like human apolipoproteins A-I and apoA-IV, in solution chicken apoA-IV adopts a loosely folded conformation (11, 12, 14, 33), or "molten globular" state (39).

Although the circular dichroism spectroscopic studies found that the secondary structure and stability of chicken apoA-IV more closely resemble those of human apoA-I, fluorescence spectroscopy revealed several features that suggest its tertiary structure resembles that of human apoA-IV. Chemical denaturation of chicken apoA-IV yielded a multiphasic red shift and a 65% increase in quantum yield that preceded loss of secondary structure. We have proposed that these fluorescence characteristics denote the presence of stable unfolding intermediates (perhaps unfolding of more hydrophilic, less stable helices) and a loosely folded native conformation that places the amino-terminal Trp-12 within a confluence of hydrophobic helices, such that unfolding decreases intramolecular tryptophan–tyrosine energy transfer (33). The present finding that the tryptophan emission in apoA-IVΔC44 was red shifted to 338 nm suggests that the C terminus may participate in this conformation. Local unfolding without global loss of secondary structure could facilitate reversible binding of apoA-IV to lipid interfaces, analogous to the interfacial behavior of the insect lipid-binding protein, Lp-III (40).

ApoA-IV has the weakest lipid affinity (11, 13, 14) and lowest interfacial exclusion pressure (15) of any apolipoprotein, and its labile binding to lipoproteins is sensitive to processes that alter interfacial pressure and lipid packing of the lipoprotein surface (36). We have proposed that this behavior is a consequence of its high content of hydrophilic α helices (9) that are incapable of deeply penetrating lipid monolayers (11), so that with increasing surface pressures these helices are sequentially excluded from the interface (15). Thus the observation that chicken apoA-IV has a higher interfacial exclusion pressure than human apoA-IV is in keeping with its relatively greater hydrophobicity. However, the slow binding kinetics of both chicken and human apoA-IV to DMPC vesicles, in comparison with apoA-I, suggests that the α helices in these

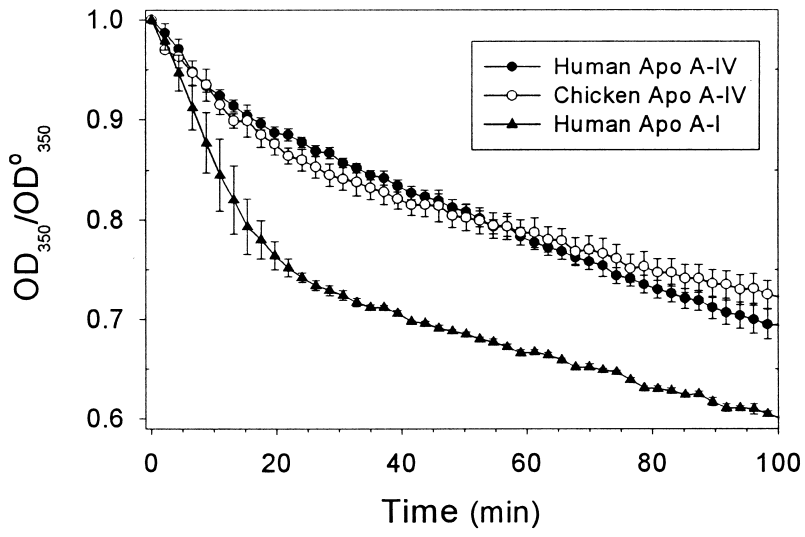

Fig. 7. Binding of chicken apolipoprotein A-IV and human apolipoproteins A-IV and A-I to dimyristoyl phosphatidylcholine. The optical density of a solution of DMPC multilamellar vesicles was continuously monitored at 350 nm after addition of apolipoproteins at a 1:50 protein/lipid ratio. Data points are the means ± SE for four (chicken apoA-IV) or five (human apoA-I and apoA-IV) experiments.

apoproteins have lost the ability to deeply penetrate lipid interfaces (15, 37).

Gene sequence analysis predicts that apoA-IV originated by reduplication of the apoA-I gene approximately 270 million (2) to 307 million years ago (6). The most recent evolution of human apoA-IV has also been suggested by the observation that there is a higher degree of similarity among the α-helical repeats in apoA-IV than in other human apolipoproteins (41). The evolution of apoA-IV from an ancestral apoA-I molecule is supported by the Fourier analysis finding of a molecular footprint of the ancient elongation site near residue 230 in the chicken and human apoA-IV sequences. It is intriguing to note that the proposed evolutionary time frame for the appearance of apoA-IV coincides exactly with the divergence of the synapsids, the ancestors of mammals, from the diapsids, the ancestors of birds and reptiles (42). Hence chicken apoA-IV may represent a "molecular fossil" of the early stages in the evolution of apoA-IV, which thereafter underwent further changes in structure to acquire a new function unique to the needs of mammalian lipoprotein metabolism.

In considering the biological forces that could have driven the molecular evolution of apoA-IV, it is relevant to consider two unique features of avian intestinal lipoprotein physiology. First, unlike mammals, avians do not secrete chylomicrons into mesenteric lymph during lipid absorption; rather, they secrete much smaller particles, called portomicrons, directly into portal blood (43). Second, avians lack the molecular machinery to edit apoB mRNA; hence avian intestine synthesizes only apoB-100 (44). It is worth noting in this regard that hepatic apoA-IV synthesis occurs only in those mammalian species capable of hepatic apoB mRNA editing (45). Together these observations suggest that a full-length mammalian apoA-IV may have coevolved with the appearance of apoB editing to serve some function in chylomicron assembly.

The thermodynamic requisites for chylomicron assembly (46) are the same as for the formation of an oil-in-water macroemulsion (47). As nascent chylomicrons expand with addition of core triglycerides, a mechanism is needed to lower interfacial tension (otherwise the free energy cost of expanding a hydrophobic surface would limit particle growth) but also increase interfacial elasticity (otherwise collisional forces would cause particle fusion and phase separation). The C-terminal half of apoB-100 contains two α-helical domains (48) that can adapt their surface conformation during particle growth to fulfill these functions (49). ApoB-48 lacks these domains. Thus the appearance of apoB editing may have created a need for an auxiliary protein to replace the expansile function of the lost α2 and α3 domains in apoB-100.

The interfacial properties of apoA-IV may be optimally suited for this role. Human apoA-IV displays unique interfacial elasticity (38), which suggests that its hydrophilic α helices can stabilize interfaces by moving in and out of the interface, expanding and contracting like an accordion, according to lateral pressure. This behavior is analogous to the function of the insect protein apolipophorin III in stabilizing hemolymph lipophorin particles (40). We have proposed that apoA-IV thus functions as a barostat that maintains lipoprotein surface tension within a critical range required for biological processes (15, 36). The present data suggest that these characteristics are only partially developed in chicken apoA-IV.

In summary, these studies suggest that chicken apoA-IV is a unique apolipoprotein whose biophysical properties are a hybrid between those of human apoA-I and apoA-IV. The data also support the concept that apoA-IV evolved from apoA-I, first by sequence elongation and then by structural organization of C-terminal domains and hydrophilic residue substitutions throughout the molecule, to serve a new function in mammalian lipoprotein synthesis.

The authors thank Dr. Duncan Hite for use of the Electronetics pulsating bubble surfactometer, and Wolfgang Schneider for advice and support. This research was supported by grant HL30897 from the National Heart, Lung, and Blood Institute.

Manuscript received 14 March 2000 and in revised form 11 May 2000.

REFERENCES

1. Weinberg, R. B., and A. M. Scanu. 1983. The isolation and characterization of human apolipoprotein A-IV from lipoprotein depleted serum. *J. Lipid Res.* **24:** 52–59.
2. Luo, C. C., W. H. Li, M. N. Moore, and L. Chan. 1986. Structure and evolution of the apolipoprotein multigene family. *J. Mol. Biol.* **187:** 325–340
3. Weisgraber, K. H., T. P. Bersot, and R. W. Mahley. 1978. Isolation and characterization of an apoprotein from the d < 1. 006 lipoproteins of human and canine lymph homologous with the rat A-IV apoprotein. *Biochem. Biophys. Res. Commun.* **85:** 287–292.
4. Hayashi, H., D. F. Nutting, K. Fujimoto, J. A. Cardelli, D. Black, and P. Tso. 1990. Transport of lipid and apolipoproteins apo A-I and apo A-IV in intestinal lymph of the rat. *J. Lipid Res.* **31:** 1613–1625.
5. Green, P. H., R. M. Glickman, J. W. Riley, and E. Quinet. 1980. Human apolipoprotein A-IV: intestinal origin and distribution in plasma. *J. Clin. Invest.* **65:** 911–919.
6. Wang, L., J. H. Chai, Y. Lu, and C. C. Tan. 1994. Studies on the molecular evolution of apolipoprotein multigene family. 1994. *Acta Genet. Sinica.* **21:** 81–95.
7. Kalogeris, T. J., M. D. Rodriquez, and P. Tso. 1997. Control of synthesis and secretion of intestinal apolipoprotein A-IV. *J. Nutr.* **127:** 537S–543S.
8. Weinberg, R. B. 1994. Identification of functional domains in the plasma apolipoproteins by analysis of inter-species amino acid sequence variability. *J. Lipid Res.* **35:** 2212–2222.
9. Weinberg, R. B. 1987. Differences in the hydrophobic properties of discrete alpha helical domains of rat and human apolipoprotein A-IV. *Biochim. Biophys. Acta.* **918:** 299–303.
10. Segrest, J. P., M. K. Jones, H. De Loof, C. G. Brouillette, Y. V. Venkatachalapathi, and G. M. Anatharamaiah. 1992. The amphipathic helix in exchangeable apolipoproteins: a review of secondary structure and function. *J. Lipid Res.* **33:** 141–166.
11. Weinberg, R. B., and M. Jordan. 1990. Effects of phospholipid on the structure of human apolipoprotein A-IV. *J. Biol. Chem.* **265:** 8081–8086.
12. Weinberg, R. B., M. Jordan, and A. Steinmetz. 1990. Distinctive structure and function of human apolipoprotein variant, Apo A-IV-2. *J. Biol. Chem.* **265:** 18372–18378.
13. Weinberg, R. B., and M. S. Spector. 1985. Human apolipoprotein A-IV: displacement from the surface of triglyceride-rich particles by HDL2-associated C-apoproteins. *J. Lipid Res.* **26:** 26–37.
14. Weinberg, R. B., and M. S. Spector. 1985. Structural properties and lipid binding of human apolipoprotein A-IV. *J. Biol. Chem.* **260:** 4914–4921.
15. Weinberg, R. B., J. A. Ibdah, and M. C. Phillips. 1992. Adsorption

of apolipoprotein A-IV to phospholipid monolayers spread at the air/water interface. *J. Biol. Chem.* **267:** 8977–8983.
16. Reue, K., and T. Leete. 1991. Genetic variation in mouse apolipoprotein A-IV due to insertion and deletion in a region of tandem repeats. *J. Biol. Chem.* **266:** 12715–12721.
17. Hixson, J. E., C. M. Kammerer, G. E. Mott, M. L. Britten, S. Birnbaum, P. K. Powers, and J. L. VandeBerg. 1993. Baboon apolipoprotein A-IV. Identification of Lys(76)→Glu that distinguishes two common isoforms and detection of length polymorphisms at the carboxyl terminus. *J. Biol. Chem.* **268:** 15667–15673.
18. Lohse, P., M. R. Kindt, D. J. Rader, and H. B. Brewer. 1990. Genetic polymorphism of human plasma apolipoprotein A-IV is due to nucleotide substitutions in the apolipoprotein A-IV gene. *J. Biol. Chem.* **265:** 10061–10064.
19. Lohse, P., M. R. Kindt, D. J. Rader, and H. B. Brewer. 1990. Human plasma apolipoproteins A-IV-0 and A-IV-3: molecular basis for two rare variants of apolipoprotein A-IV-1. *J. Biol. Chem.* **265:** 12734–12739.
20. Weinberg, R. B. 1999. The apolipoprotein A-IV-2 allele: association of its worldwide distribution with adult persistence of lactase and speculation on its function and origin. *Genet. Epidemiol.* **16:** 285–297.
21. Williams, S. C., S. G. Grant, K. Reue, B. Carrasquillo, A. J. Lusis, and A. J. Kinniburgh. 1989. Cis-acting determinants of basal and lipid-regulated apolipoprotein A-IV expression in mice. *J. Biol. Chem.* **264:** 19009–19016.
22. McCombs, R. J., D. E. Marcadis, J. Ellis, and R. B. Weinberg. 1994. Attenuated hypercholesterolemic response to a high cholesterol diet in subjects heterozygous for the apolipoprotein A-IV-2 allele. *N. Engl. J. Med.* **331:** 706–710.
23. Mata, P., J. M. Ordovas, J. Lopez-Miranda, A. H. Lichtenstein, B. Clevidence, J. T. Judd, and E. J. Schaefer. 1994. Apo A-IV phenotype affects diet-induced plasma LDL cholesterol lowering. *Arterioscler. Thromb.* **14:** 884–891.
24. Steinmetz, A., M. Hermann, J. Nimpf, R. Aebersold, A. Ducret, R. B. Weinberg, and W. J. Schneider. 1998. Expression and conservation of apolipoprotein A-IV in an avian species. *J. Biol. Chem.* **273:** 10543–10549.
25. Bartlett, G. R. 1959. Phosphorus assay in column chromatography. *J. Biol. Chem.* **234:** 466–468.
26. Weinberg, R. B., R. A. Hopkins, and J. B. Jones. 1996. *Methods Enzymol.* **263:** 282–296.
27. Duverger, N., A. Murry-Brelier, M. Latta, S. Reboul, G. Castro, J. F. Mayaux, J. C. Fruchart, J. M. Taylor, A. Steinmetz, and P. Denefle. 1991. Functional characterization of human recombinant apolipoprotein AIV produced in Escherichia coli. *Eur. J. Biochem.* **201:** 373–383.
28. Shore, B., and V. Shore. 1969. Isolation and characterization of polypeptides of human serum lipoproteins. *Biochemistry.* **8:** 4510–4516.
29. Smith, P. K., R. I. Krohn, G. T. Hermanson, A. K. Mallia, F. H. Gartner, M. D. Provenzano, E. K. Fujimoto, N. M. Goeke, B. J. Olson, and D. C. Klenk. 1985. Protein assay using bicinchoninic acid. *Anal. Biochem.* **150:** 76–85.
30. Finer-Moore, J., and R. M. Stroud. 1984. Amphipathic analysis and possible formation of the ion channel in an acetylcholine receptor. *Proc. Natl. Acad. Sci. USA.* **81:** 155–159.
31. Eisenberg, D. 1984. Three-dimensional structure of membrane and surface proteins. *Annu. Rev. Biochem.* **53:** 595–623.
32. Tall, A. R., G. G. Shipley, and D. M. Small. 1976. Conformational and thermodynamic properties of apo A-1 of human high density lipoproteins. *J. Biol. Chem.* **251:** 3749–3755.
33. Weinberg, R. B. 1988. Exposure and electronic interaction of tyrosine and tryptophan residues in human apolipoprotein A-IV. *Biochemistry.* **27:** 1515–1521.
34. Enhorning, G. 1977. Pulsating bubble technique for evaluating pulmonary surfactant. *Appl. Physiol.* **43:** 198–203.
35. Benjamins, J., A. Cagna, and E. H. Lucassen-Reynders. 1996. Viscoelastic properties of triacylglycerol/water interfaces covered with proteins. *Colloids Surfaces.* **114:** 245–254.
36. Weinberg, R. B., V. R. Cook, P. Kussie, and A. R. Tall. 1994. Interfacial properties of recombinant human cholesterol ester transfer protein. *J. Biol. Chem.* **269:** 29588–29591.
37. Pownall, H. J., J. B. Massey, S. K. Kusserow, and A. M. Gotto. 1978. Kinetics of lipid-protein interactions: interaction of apolipoprotein apo A-I from human plasma high density lipoproteins with phosphatidylcholines. *Biochemistry.* **17:** 1183–1188.
38. Weinberg, R. B., V. R. Cook, J. A. DeLozier, and G. S. Shelness. 2000. Dynamic interfacial properties of human apolipoproteins A-IV and B-17 at the air/water and oil/water interface. *J. Lipid Res.* **41:** 1419–1427.
39. Gursky, O., and D. Atkinson. 1996. Thermal unfolding of human high-density apolipoprotein A-I: implications for a lipid-free molten globular state. *Proc. Natl. Acad. Sci. USA.* **93:** 2991–2995.
40. Narayanaswami, V., and R. O. Ryan. 1997. Protein-lipid interactions of apolipophorin-III, a model exchangeable amphipathic apolipoprotein. *Biochem. Soc. Trans.* **25:** 1113–1118.
41. Ponnuswamy, P. L., and S. Selvaraj. 1992. Structural similarities in the repeat sequences of plasma apolipoproteins A-I, A-IV, and E. *Protein Sequence Data Anal.* **5:** 47–56.
42. Kumar, S., and S. B. Hedges. 1998. A molecular timescale for vertebrate evolution. *Nature.* **392:** 917–920.
43. Bensadoun, A., and A. Rothfeld. 1972. The form of absorption of lipids in the chicken, *Gallus domesticus*. *Proc. Soc. Exp. Biol. Med.* **141:** 814–817.
44. Chan, L., B. H. J. Chang, M. Nakamuta, W. H. Li, and L. C. Smith. 1997. Apobec-1 and apolipoprotein B mRNA editing. *Biochim. Biophys. Acta.* **1345:** 1–26.
45. Greeve, J., I. Altkemper, J. H. Dieterich, H. Greten, and E. Windler. 1993. Apolipoprotein B mRNA editing in 12 different mammalian species: hepatic expression is reflected in low concentrations of apo B-containing plasma lipoproteins. *J. Lipid Res.* **34:** 1367–1383.
46. Shelness, G. S., M. F. Ingram, X. F. Huang, and J. A. DeLozier. 1999. Apolipoprotein B in the rough endoplasmic reticulum: translation, translocation and the initiation of lipoprotein assembly. *J. Nutr.* **129:** 456S–462S.
47. Rosen, M. J. 1989. Emulsification by surfactants. *In* Surfactants and Interfacial Phenomena. 2nd edition. John Wiley & Sons, New York. 304–322.
48. Segrest, J. P., M. K. Jones, V. K. Mishra, G. M. Anatharamaiah, and D. W. Garber. 1994. Apolipoprotein B has a pentapartite structure composed of three amphipathic α helical domains alternating with two amphipathic β strand domains: detection by the computer program LOCATE. *Arterioscler. Thromb.* **14:** 1674–1685.
49. Chauhan, V., X. Wang, T. Ramsamy, R. W. Milne, and D. L. Sparks. 1998. Evidence for lipid-dependent structural changes in specific domains of apolipoprotein B. *Biochemistry.* **37:** 3735–3742.